**M. I. Siddiqui[1*] • S. Munir[1] • M. R. Heikal[1, 2] • G. deSercey[2] • A. Rashid A. Aziz[1] • S. C. Dass[1]**

# Simultaneous velocity measurements and the coupling effect of the liquid and gas phases in slug flow using PIV-LIF technique

[1]Universiti Teknologi PETRONAS, Bandar Seri Iskandar, 31750, Perak, Malaysia
[2]University of Brighton, Brighton BN2 4GJ, UK
siddiqi_ciit2003@yahoo.com

**Abstract** The analysis of a two-phase slug flow is of immense importance due to its vast applications in many industrial problems. A number of experimental and analytical studies have been carried out to study this complex and unwanted phenomena. Mostly these studies were limited to the liquid phase and to the statistical parameters and formation mechanism. So far no attempt has been made to study the phase interaction and coupling effects of both phases simultaneously, which is more important in understanding this complex flow behaviour. This kind of study requires the instantaneous velocity fields of both phases simultaneously. Therefore, in this study a PIV-LIF technique has been applied to study two-phase (liquid-gas) slug flow in a lab facility. Water and gas were considered as working fluids, and slug flow was generated in a nearly horizontal pipe with an inclination of 1.16° to consider the terrain slugging mechanism. Liquid and gas phases were seeded simultaneously with fluorescent and titanium dioxide tracer particles respectively. Two CCD cameras installed with low pass and band pass filters were used to capture images for separate phases. Instantaneous velocity field for both liquid and gas phases were measured simultaneously. To extract the coherent structures and for the analysis of turbulence in liquid and gas phase the proper orthogonal decomposition (POD) analysis technique was applied to the velocity fields. Large energy containing modes were successfully revealed by POD. The energy distribution of spatial modes for both phases was also measured and compared.

**Keywords** PIV-LIF · simultaneous velocity · pipe flow · slug flow · POD

## 1 Introduction

Multiphase flows and especially slug flows have applications in numerous industries such as oil and gas transportation, nuclear cooling, cryogenics, steam generation, etc. Since slug flow can have potentially catastrophic effects on pipes structure it is the subject of many experimental techniques, which can be classified either as intrusive or as non-intrusive. The most widely used non-intrusive technique is Particle Image Velocimetry (PIV). It is a laser optical technique used for the measurement of instantaneous velocity flow fields. The flow is seeded with suitable tracer particles which are assumed to follow the flow faithfully. These particles scatter light when illuminated by means of a laser. A CCD camera, synchronised to the laser, captures several images of the light scattered by each particle within a short time interval. The unit displacement of the particles can then be computed from successive images by means of cross-correlation. Finally, the local velocity is obtained by dividing the displacement over the time interval between the laser pulses (Adrian 2011).

### 1.1 Application of PIV in Multiphase Flows

PIV is commonly applied to single phase flows. In multiphase flows, measuring the velocity of both phases simultaneously remains challenging and significant. A new experimental procedure for performing simultaneous phase-separated velocity measurements in two-phase flows was introduced by Lindken and Merzkrich (2002). Particle Image Velocimetry in combination with Laser Induced Fluorescence (LIF) and pulse shadowgraph were used to measure simultaneously the instantaneous velocities of the liquid phase and bubbles together with the bubbles' shape. This technique was however restricted to the bubbly flow regime. Further, Fujiwar et al. (2004) used PIV in combination with LIF and double shadow projection technique to measure the shape and the motion of the bubble rising in a rectangular channel. Three CCD cameras were used at different positions, one for velocity measurements and two for bubble shadow images. Velocity near the vicinity of the bubble and the 3D vortex structures were studied simultaneously. Similarly, the simultaneous velocity measurement of the liquid and the micro bubbles was studied in

Published in Journal of Visualization
DOI 10.1007/s12650-015-0302-1
The final publication is available at link.springer.com

a horizontal channel using PIV-LIF in combination with Particle Tracking Velocimetry (PTV) and Shadow Image Technique (SIT) by Kitagawa et al. (2005). Moreover, to visualize and to measure the vortex structures in large shear layers of the jet and the bubbles Milenković et al. (2009) used PIV-LIF in combination with a back light photographic recording technique. Jirka et al. (2010) used PIV-LIF to study the grid-stirred induced and boyant convective turbulence at an air-water interface. Further use of PIV-LIF in combination with shadowgraph was seen in the simultaneous study of liquid phase and bubble velocity in a vertical channel flow (Joshi et al. 2010). Irrespective of the liquid and gas flow PIV-LIF is also efficient to measure the simultaneous velocity field of solid and gas flows. An Aeolian sediment transport was studied in a wind-sand flow using PIV-LIF and velocity of both phases was measured by Wang et al. (2011).

### 1.2 Application of PIV in Slug Flows

Despite slug flow regime being one of the most important in liquid gas flow, optical measurement studies of this regime are scarce. However, Goharzadeh and Rodgers (2009) measured the instantaneous velocity field of the liquid phase in a slug flow using PIV. They compared the velocity field of a slugy body in a film region and noticed a significant drop of velocity in that region. Also, Cameiro et al. (2011) applied PIV-LIF and Pulse Shadow Technique (PST) on a horizontal slug. They measured the velocity field of liquid phase, slug frequency and slug length. Czapp et al. (2012) successfully applied high-speed Stereo PIV along with LIF on a horizontal pipe slug flow. 3D velocity fields and volumetric fraction for the liquid phase were measured. The influence of the gas phase on the dynamics of a slug flow has been examined by Siddiqui et al. (2014) using PIV and the detailed turbulence analysis of the liquid phase in slug flow has been carried out using PIV and Proper Orthogonal Decomposition (POD) by Munir et al. (2014). None of these studies, however, have attempted to measure the full velocity fields of both phases simultaneously and to examine their micro structure and interactions. A complete understanding of the interaction between both phases requires the instantaneous measurements of the full flow fields simultaneously.

In this study, a new approach using PIV-LIF technique is introduced to measure the instantaneous velocity fields of the two-phase (liquid-gas) slug flow simultaneously. The technique was successfully applied in the lab to investigate the influence of the gas phase on the liquid phase and to study the coupling effect of the two-phases in a slug flow. Also this technique allows the turbulent analysis of both phases by using POD technique.

## 2 Methodology

### 2.1 Experimental Facility

Figure 1 depicts the schematic diagram of the experimental apparatus used for this study. The setup shown consists of a 6 m long transparent Plexiglas pipe having an internal diameter of 74 mm. The pipe was kept at an inclination of about 1.16° to represents the offshore terrain slugging mechanism. The mixing occurs in a T-shaped section with the gas-phase entering horizontally along the transparent pipe and the liquid phase entering from the bottom, as illustrated by Figure 2. Air and water were the working fluids. An air compressor with a maximum working pressure of 8 bar was used to inject the air through a nozzle with an inner diameter of 2 mm. A powder seeding generator with up to 10 bar working back-pressure was used to seed solid tracer particles in the gas phase. A mass flow meter was installed to measure the gas flow rate. A centrifugal pump with a maximum flow rate of 500 l/min was used to circulate water into the closed flow loop from a tank having capacity of 800 litres. A turbine mass flow meter was installed to measure the liquid flow rate. The flow loop was equipped with a USB acquisition and control system to operate the loop with a computer.

The test section where the optical measurements were performed was situated 3.5 m away from the inlet, allowing any effect from the T-section to dissipate. A rectangular correction box filled with the same working fluid is mounted around the test section to minimize the optical distortion caused by the curvature of the pipe.

Published in Journal of Visualization
DOI 10.1007/s12650-015-0302-1
The final publication is available at link.springer.com

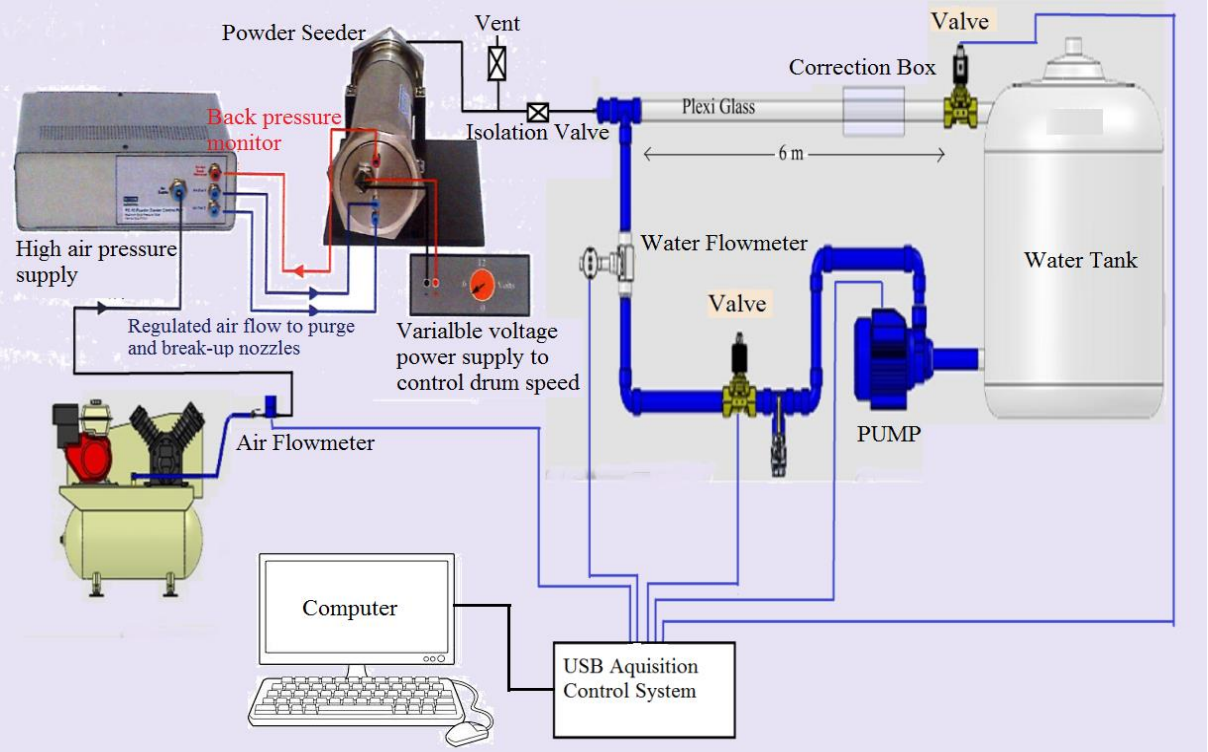


**Fig. 1** Schematic of the experimental lab facility for two-phase pipe flow

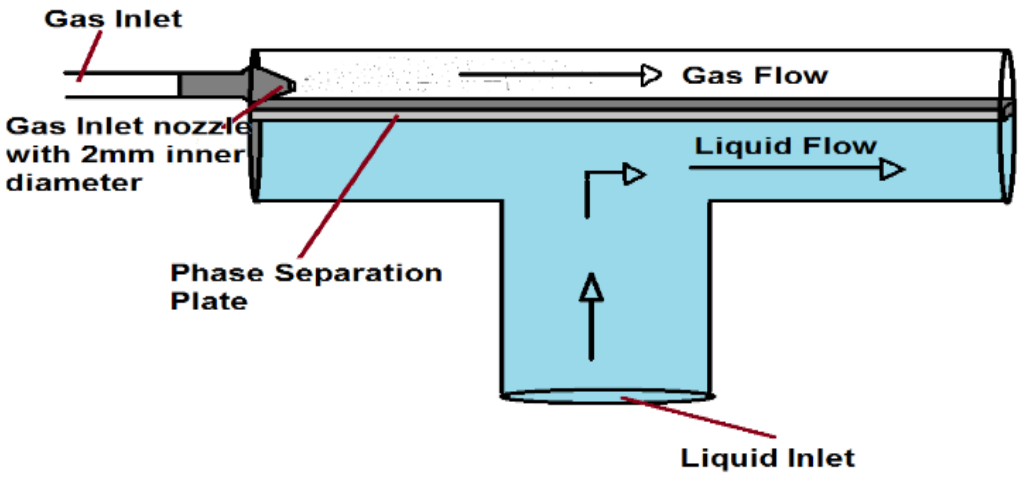


**Fig. 2** The T-shaped mixing zone installed with a horizontal plate to separate the phases initially

2.2 Measurement Technique

A slug flow regime in the lab apparatus was generated for the optical diagnostic measurements at flow rates of 100 l/min and 80 l/min for the gas and liquid respectively. The inlet Reynolds number for the liquid and gas phases were considered to be 35752 and 1518 respectively. Particle Image Velocimetry (PIV) along with Laser Induced Fluorescence (LIF) was used to measure the velocity field of the gas and liquid phases simultaneously.

Published in Journal of Visualization
DOI 10.1007/s12650-015-0302-1
The final publication is available at link.springer.com

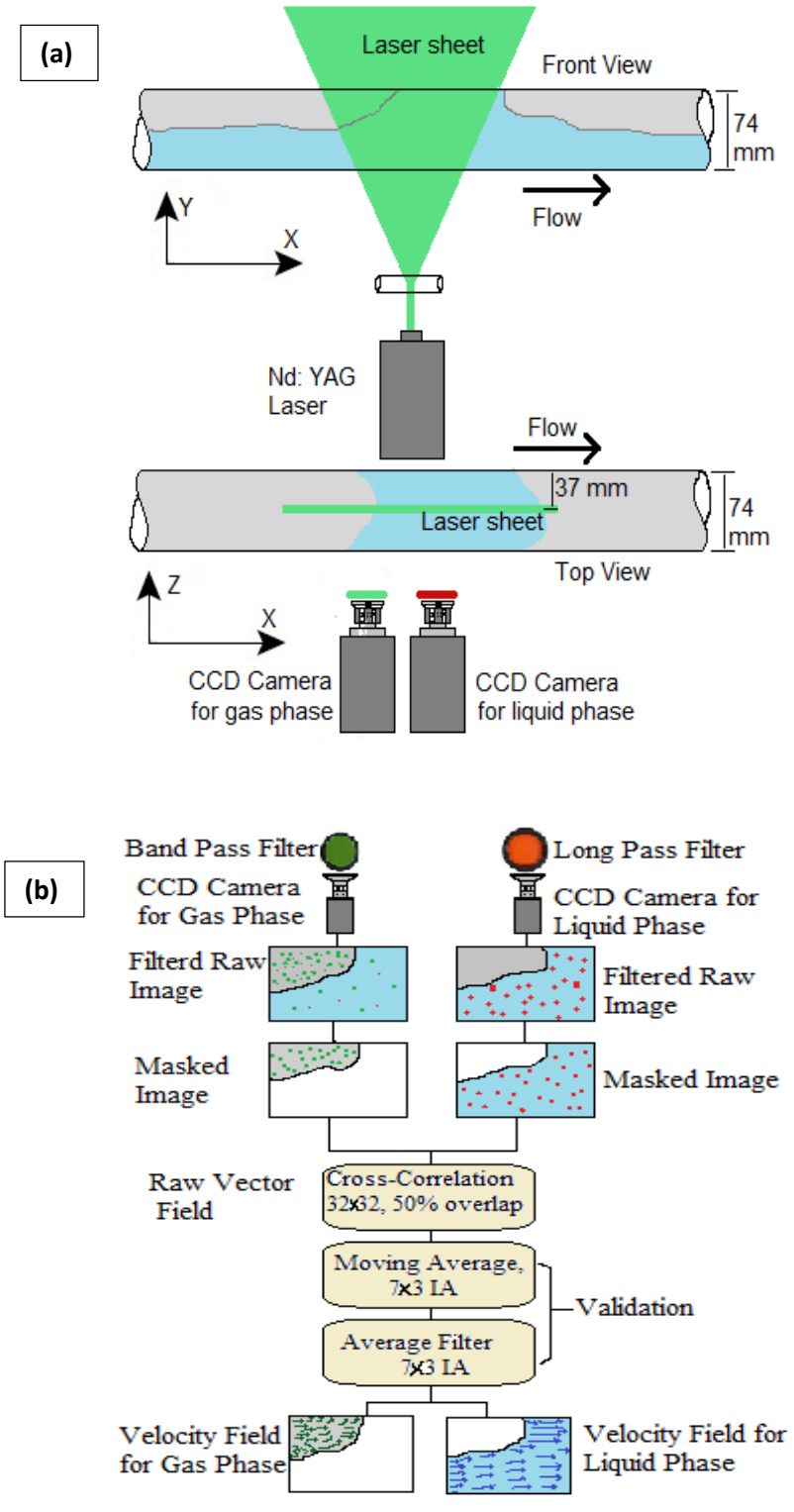


**Fig. 3 a** Camera and laser setup for optical measurements. **b** Schematic diagram of the PIV-LIF technique to measure the simultaneous velocity fields of the gas and liquid phases

Published in Journal of Visualization
DOI 10.1007/s12650-015-0302-1
The final publication is available at link.springer.com

Figure 3(a, b) shows the schematic diagram of the PIV-LIF setup for the phase separated velocity measurements. The liquid phase was seeded with Rhodamine-B coated spherical shaped polymer particles (methyl methacrylate) having a mean diameter of 20 µm, density 1.19 g/cm$^3$, and a refractive index of 1.479. A solid powder seeder was used to seed the air phase with Titanium Dioxide ($TiO_2$) tracer particles of mean diameter 0.3 µm, density 4.2 g/cm$^3$ and refractive index 2.6. These particles were then illuminated by means of a double pulsed Nd-YAG laser of wavelength 532 nm pulsing at a frequency of 15 Hz and maximum energy of 500 mJ/5 ns pulse. The laser sheet was positioned in the mid plane of the test section. When illuminated with the laser, the fluorescent particles scattered orange light at a wavelength of 555-590 nm, whereas the $TiO_2$ particles scattered at the same wavelength as the laser (532 nm). To differentiate the signal from the liquid and gas phases, two 12-bit HiSense CCD (charged couple device) cameras with resolution of 1344 × 1024 pixels were positioned perpendicularly to the laser sheet. The cameras were equipped with optical filters, the gas phase camera with a band pass filter centered at 532 nm with a FWHM of 20 nm, the liquid phase camera with a long pass filter with a cut off wavelength of 570 nm. The purpose of the filters was to completely remove the signal from the other phase.

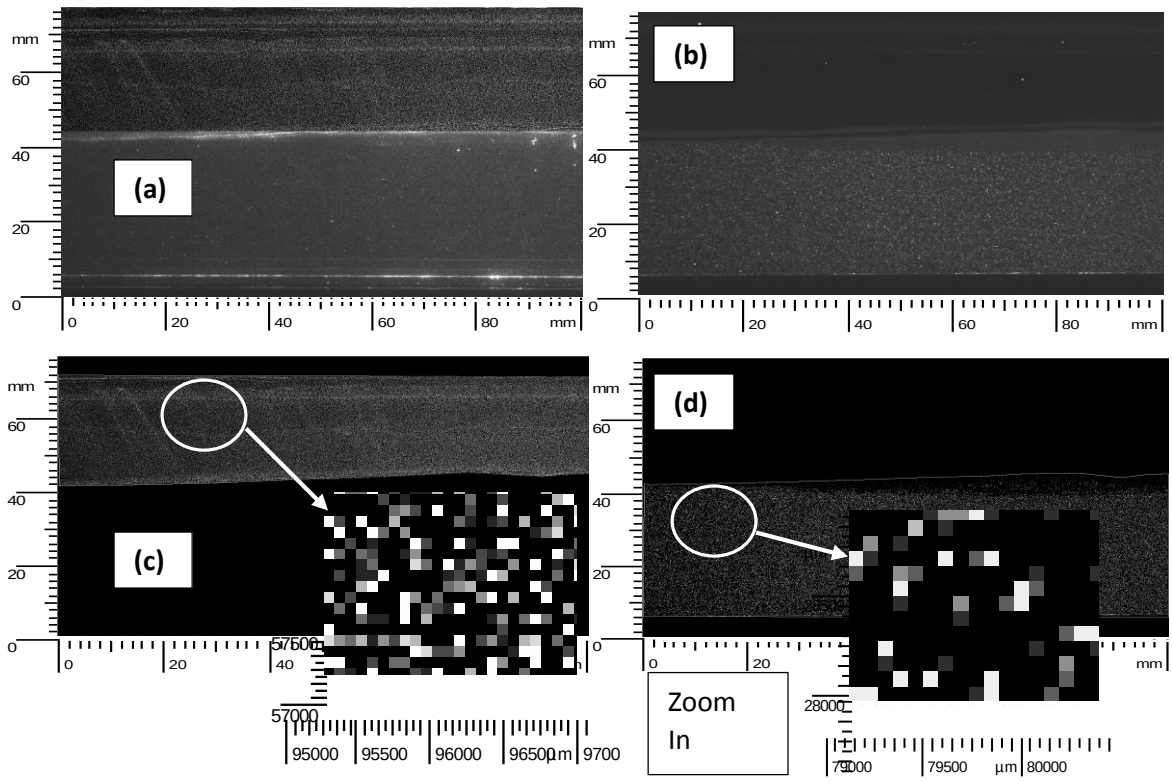


**Fig. 4** The raw images of **a** gas and **b** liquid phase with **c, d** the same after masking. A zoomed in section highlighting the particles is shown beneath

A minimum of 200 image pairs were captured with each camera and processed using Dantec Dynamic Flow manager. Figure 4(b) shows the image captured using the long pass filter (liquid phase) and it can be seen that the filter effectively removed the signal from the gas phase. Figure 4(a) shows the image captured using the band pass filter for the gas phase. This filter effectively removed the signals from the liquid particles but for some small cross talk from the liquid particles due to Mie scattering. However, this Mie signal is weaker than the Mie signal of the gas particle as most of the laser energy is absorbed by the fluorescence process instead of being scattered. In any case, the interface between the liquid and gas can be identified clearly in the images and the liquid phase can be masked in the gas image. There is also a small amount of diffusion of the gas particle in the liquid phase. These show a strong signal on the gas image, but once again they can be masked by removing the liquid phase, fig. 4(c).

Published in Journal of Visualization
DOI 10.1007/s12650-015-0302-1
The final publication is available at link.springer.com

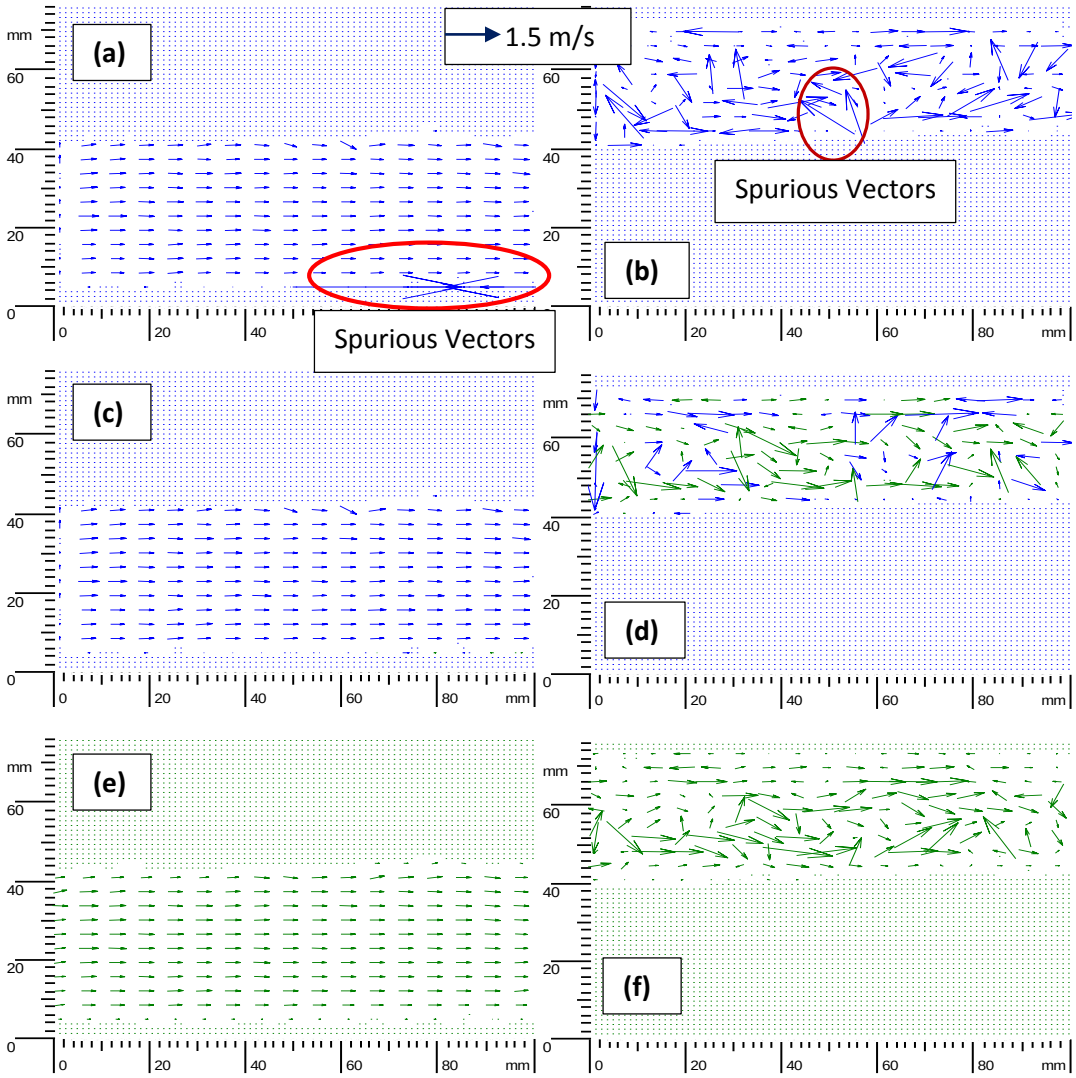


**Fig. 5** Spurious vectors after cross-correlation can be removed by applying a moving average filter and further validations can be done by using an average filter for **a, c, e** liquid and **b, d, f** gas vector fields

Images were first masked to remove the cross-talk, figure 4(c-d) then a standard cross-correlation PIV algorithm was applied using 50% overlap and a fixed interrogation area (IA) of 32×32 pixels. Spurious vectors were finally removed using a moving average filter and average filter of 7×3 IA. This resulted in a maximum of 83 × 63 vectors per image, figure 5(a-f).

## 3 Results and Discussion

### 3.1 Simultaneous Velocity Fields of Liquid and Gas Phase and Velocity Profiles

To study the dynamic parameters of a slug flow, three main sections (Slug Nose, Slug Wake and Film region) were targeted for visualization. Figure 6 gives the entire velocity fields for the liquid and gas phases at the different sections of a slug flow, whereas the scalar distribution of the velocity fields for the two phases are given in figure 7. Both figures 7 and 8 shows that a low velocity profile can be seen in the stretched liquid film region as most of the mass has been displaced by the slugy body. The gas velocity inside the long bubble in this section remains dominant and the average gas velocity remains twice as that of the liquid phase. Some circular motion can also be seen in the gas

Published in Journal of Visualization
DOI 10.1007/s12650-015-0302-1
The final publication is available at link.springer.com

phase near both boundaries (wall and interface) due to strong shear rate. Since the gas bubble moves faster than the liquid it influences the liquid velocity in the slug wake section more significantly, as a result the upstream velocity becomes nearly equal to the gas velocity.

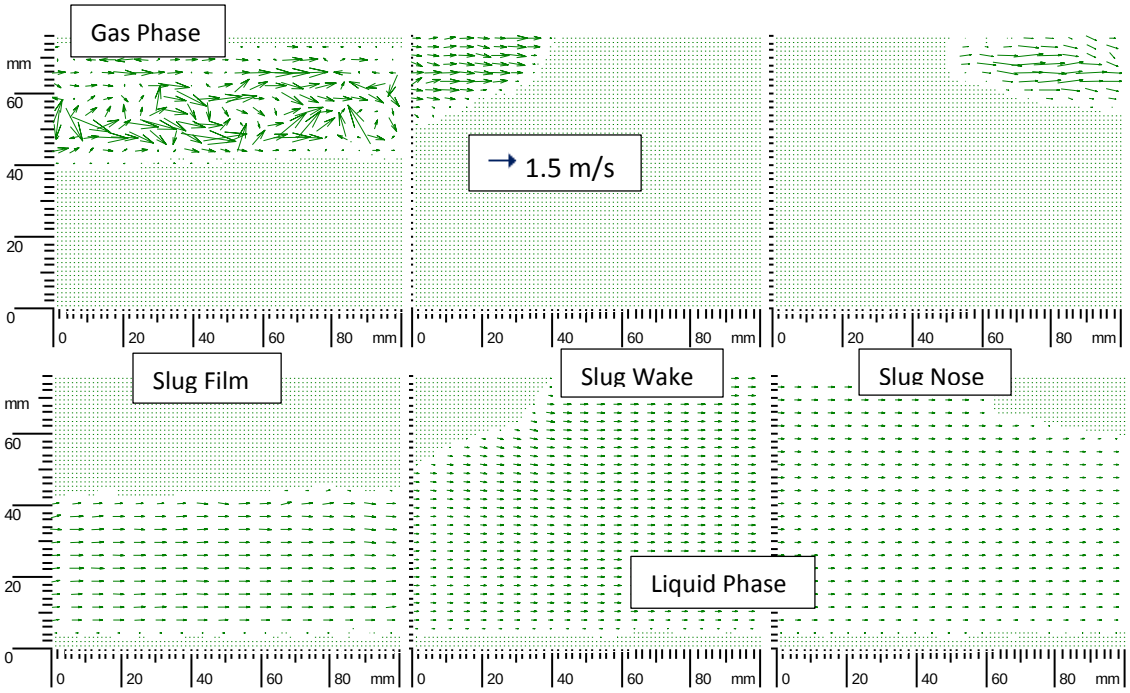


**Fig. 6** Full instantaneous velocity fields of the gas and liquid phases at three different sections of a slug flow (film, wake and nose)

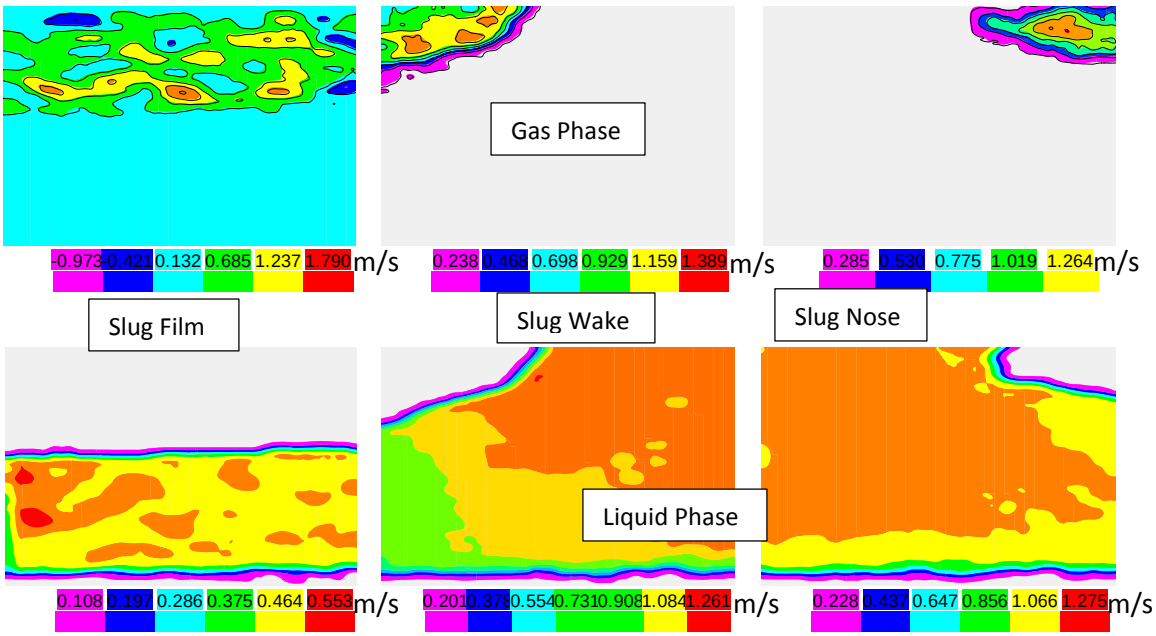


**Fig. 7** Scalar distribution of the axial velocity at different section of a unit slug. Whereas, the color scale is in m/s

Published in Journal of Visualization
DOI 10.1007/s12650-015-0302-1
The final publication is available at link.springer.com

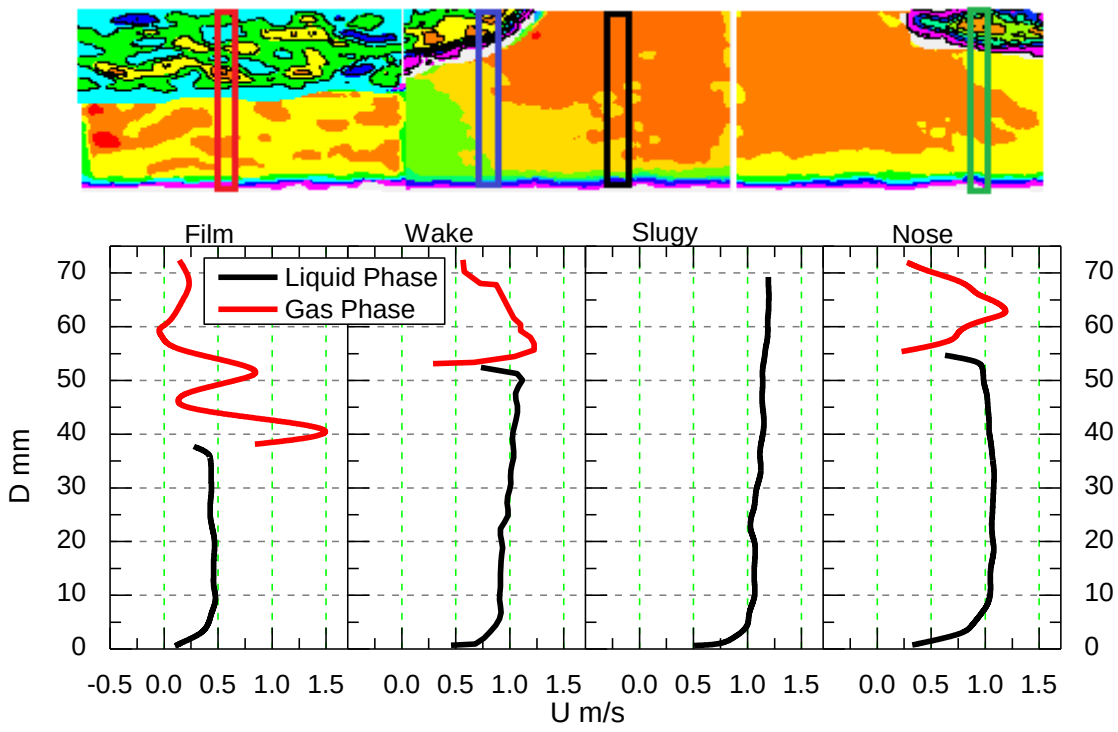


**Fig. 8** Axial velocity profiles of both (liquid and gas) phases against pipe diameter (D) at different sections in unit slug, whereas the position of measurements are shown above in a color map that is a combination of both phases shown in Fig. 7

3.2 Average Velocity, Turbulence Intensity and Vorticity

Figure 9 (a) shows the average velocity profile of the film region in a unit slug, whereas the turbulence I ntensity,

$$TI = \frac{\acute{U}}{\bar{U}} \tag{1}$$

where $\acute{U}$ is the root mean square of the fluctuating velocity and $\bar{U}$ is the mean velocity, is given in figure 9(b). Vorticity is the rotation rate of the fluid and is also known as a pseudovector field that represents the fluid's local spinning motion around a point. For a three dimensional vector field the vorticity is defined by:

$$curl\ V = \nabla \times V = \left(\frac{\partial v_z}{\partial y} - \frac{\partial v_y}{\partial z}\right)\underset{i}{\rightarrow} + \left(\frac{\partial v_x}{\partial z} - \frac{\partial v_z}{\partial x}\right)\underset{j}{\rightarrow} + \left(\frac{\partial v_y}{\partial z} - \frac{\partial v_x}{\partial y}\right)\underset{k}{\rightarrow}, \tag{2}$$

where V is the velocity vector and $\underset{i}{\rightarrow}, \underset{j}{\rightarrow} and\ \underset{k}{\rightarrow}$ are the unit vectors in x, y and z axis. In 2-D PIV velocity measurements the $\nabla \times V$ is a one-dimensional vector perpendicular on the xy-plane represented by its scalar value.The vorticity profile for both phases in the film region is shown in figure 10. The spinning motion in the gas phase is significantly higher than the liquid phase as highlighted by the vorticity profile. Moreover, the vorticity near the interface is relatively lower in the film region compared to the wake and nose sections.

Published in Journal of Visualization
DOI 10.1007/s12650-015-0302-1
The final publication is available at link.springer.com

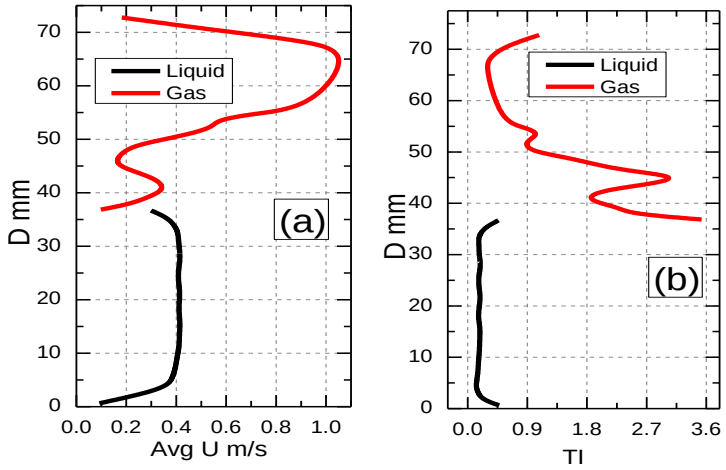


**Fig. 9 a** mean axial velocity profile, and **b** turbulent intensity profile in a film region

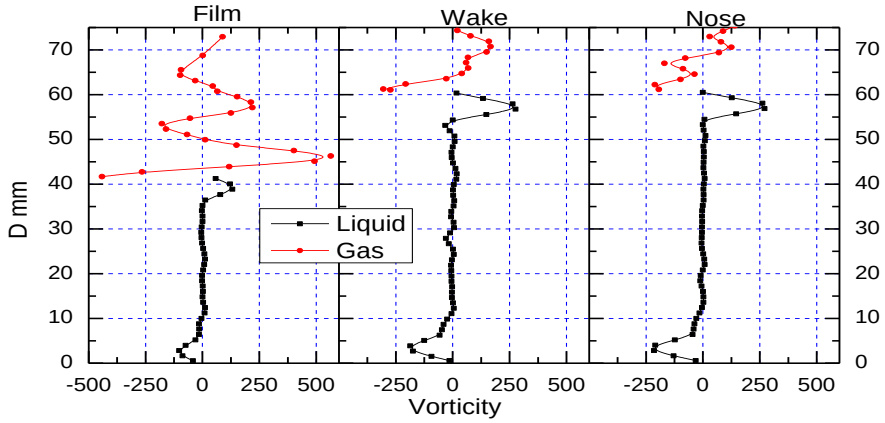


**Fig. 10** Vorticity profile in three sections of a slug flow showing the coupling of the phases

3.3 Interface Shear Stress

Figure 11 represents the coupling of both phases in terms of shear stress at the interface. The interface shear stress ($\tau = \mu \frac{\partial U}{\partial y}, where\ y \rightarrow interface$ ) was measured at two section of the slug flow (film region and bubble front). It can be seen that the shear stresses are balanced at the gas liquid interface.

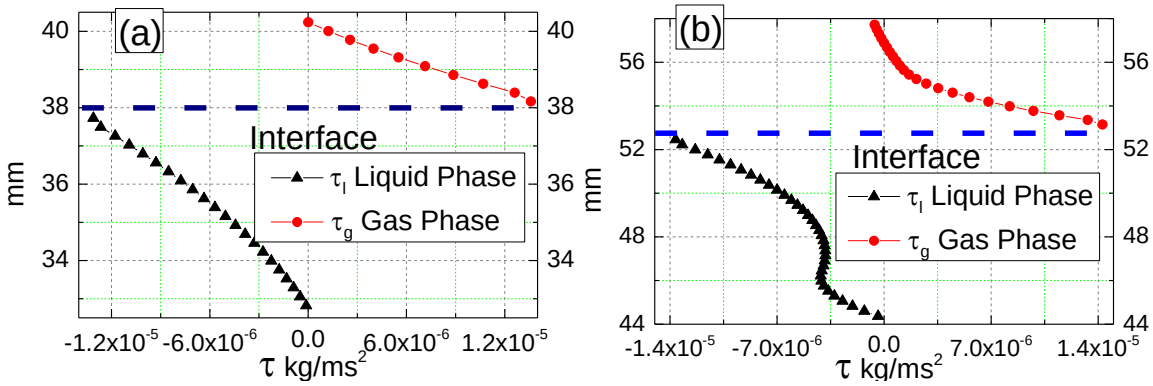


Published in Journal of Visualization
DOI 10.1007/s12650-015-0302-1
The final publication is available at link.springer.com

**Fig. 11** Interface shear stress in **a** film section, and **b** wake section

3.4 Turbulent Analysis of a Slug Flow using Proper Orthogonal Decomposition

Proper Orthogonal Decomposition (POD) was proposed by Sirovich (1987) as an objective method to identify deterministic features in turbulent flows. The flow field when decomposed into orthogonal spatial and temporal modes reveals the basic flow structures and energy content. In this technique the structure $\boldsymbol{\phi}(\boldsymbol{x})$ is identified from the flow with the largest projection onto the velocity field $\boldsymbol{u}(\boldsymbol{x}, t)$. This maximization problem leads to an eigenvalue problem

$$\int_{\boldsymbol{x}} R(\boldsymbol{x}, \boldsymbol{x}')\, \boldsymbol{\phi}_j^n(\boldsymbol{x}') d\boldsymbol{x}' = \lambda^n \boldsymbol{\phi}_j^n(\boldsymbol{x}) \tag{3}$$

Where $\lambda_j$ is the $j$th eigenvalue and presents the energy contained in the $j$th POD eigenmode $\boldsymbol{\phi}_j(\boldsymbol{x})$. $R(x, x')$ is the two-point spatial correlation tensor,

$$R(\boldsymbol{x}, \boldsymbol{x}') = \langle \boldsymbol{u}(\boldsymbol{x}, t) \boldsymbol{u}(\boldsymbol{x}', t) \rangle \tag{4}$$

Where $\langle\, . \,\rangle$ represents the ensemble average. The deviations from the mean (fluctuating velocity field) is projected onto the POD eigenmodes $\boldsymbol{\phi}_j(\boldsymbol{x})$:

$$\boldsymbol{u^n}(\boldsymbol{x}, t) = \sum_{j=1}^{J} a_j^n(t)\, \boldsymbol{\phi}_j^n(\boldsymbol{x}) \tag{5}$$

where $j$ is the mode index and $n$ is the snapshot number. The coefficients are calculated as:

$$a_j^n(t) = \int_{\boldsymbol{\Omega}} \boldsymbol{u}^n(\boldsymbol{x}, t)\, \boldsymbol{\phi}_j^n(\boldsymbol{x}) \tag{6}$$

Where Ω is the domain under consideration. The coefficients are uncorrelated to one another and in time,

$$\langle a^n(t) a^m(t) \rangle = \lambda^n \delta_m^n \tag{7}$$

Turbulent analysis of the liquid and gas phase were carried out by applying POD on the instantaneous velocity fields representing the film region of a slug flow. The flow field was decomposed into 20 spatial and temporal modes. As the spatial modes represent the dominant flow patterns that contain significant proportion of fluctuating energy, the energy distribution of both phases were measured and compared as shown in figure 12.

Published in Journal of Visualization
DOI 10.1007/s12650-015-0302-1
The final publication is available at link.springer.com

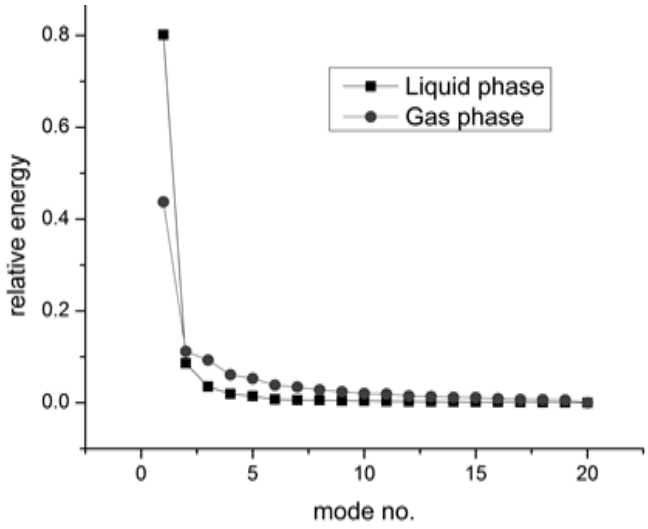


**Fig. 12** Energy spectra based on 20 numbers of snapshots

It was noticed that for the liquid phase mode 1 contains 80% of the energy on its own. Mode 2 and 3 contained 14% and 12% of the energy respectively and mode 4 has 4.2%. Mode 20 with less than 1% of the energy represents information about the presence of small vortices. From figure 12, it can also be seen that the first spatial mode of the gas contains 45% of the total energy. The bulk of the energy is dissipated by mode 9. The fluctuating energy is uniformly dissipated among the gas modes, whereas the energy dissipates more rapidly in the liquid phase than the gas phase.

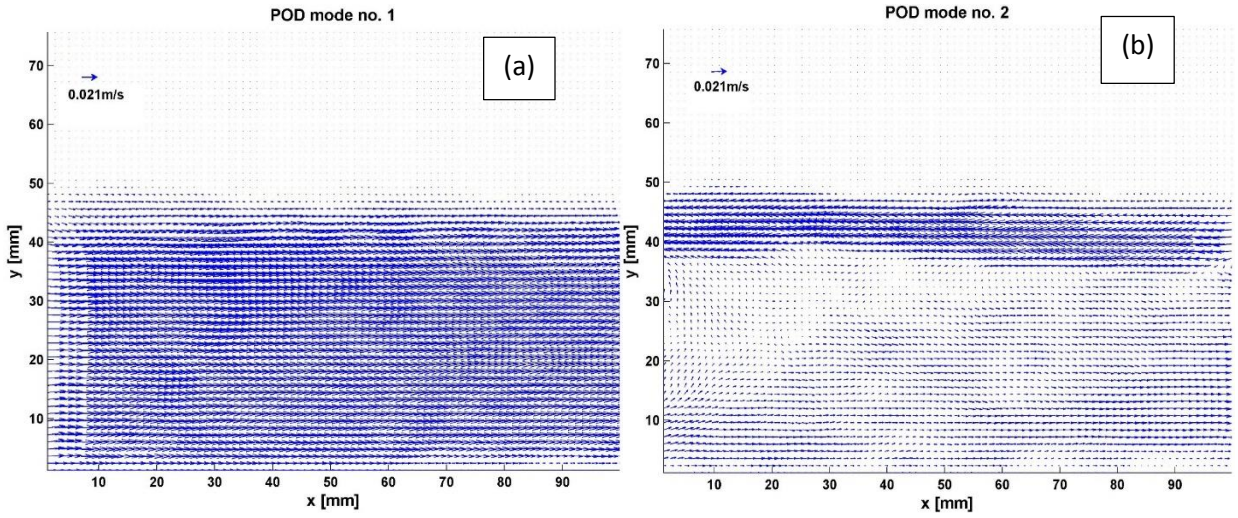


**Fig. 13** POD analysis of liquid phase, **a** spatial mode 1, and **b** spatial mode 2

Published in Journal of Visualization
DOI 10.1007/s12650-015-0302-1
The final publication is available at link.springer.com

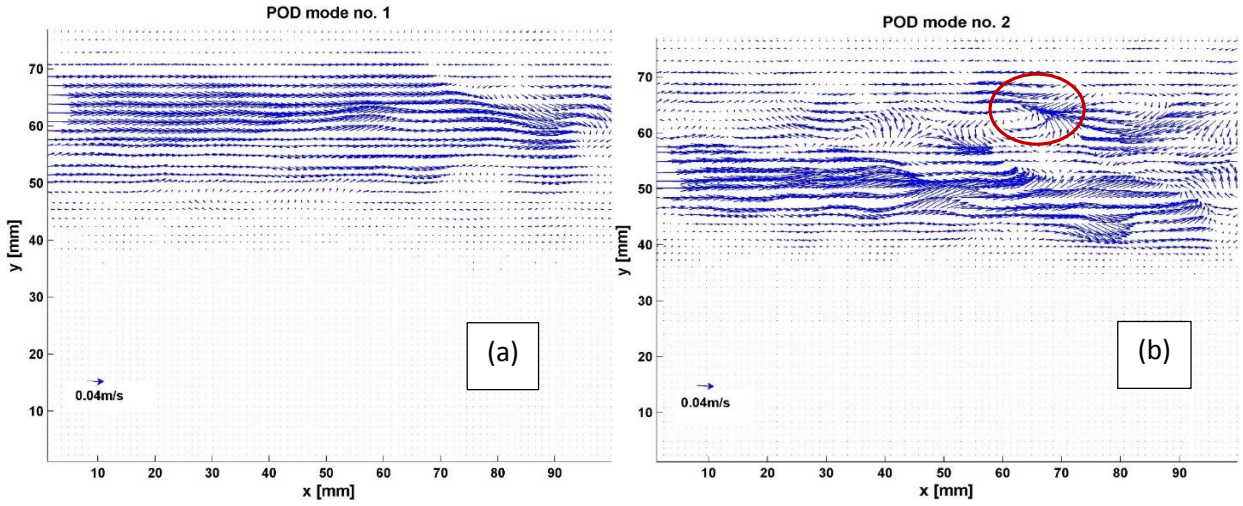


**Fig. 14** POD analysis of gas phase **a** spatial mode 1, and **b** spatial mode 2

Figure 13(a - b) shows POD spatial modes 1 and 2 for the liquid phase. The spatial mode 1 for the liquid phase is the highest turbulent energy mode containing 80 % of the energy. In physical terms, the mode 1 represents high positive fluctuations. On the other hand, mode 2 shows both positive and negative fluctuation vectors showing randomness. This mode 2 was influenced by positive fluctuation localized only near the interface. Figure 14(a - b) shows the POD modes 1 and 2 for the gas phase. These modes are significantly different from those of the liquid phase. The first spatial mode, in figure 14(a), shows high momentum flow moving from left to right. The second mode, figure 14(b), contains different dynamics and mixed behavior of the velocity vectors. Also one counter vortex appeared in this mode indicating the turbulent complexity of the gas phase. The more small scale vortices will appear in the higher order modes contributing less to the dynamics of the flow.

## 4 Conclusion

An experimental study using simultaneous PIV-LIF was conducted to analyze a two-phase (liquid-gas) slug flow in a nearly horizontal pipe at an inclination of $\theta = 1.16°$. The slug flow was generated at a flow rate of 100 l/min for gas and 80 l/min for liquid. The main objective of this study was to examine the coupling of both phases in terms of velocity exchange, momentum transfer, vorticity and the interface shear stress. In order to address this problem, simultaneous measurement of the velocity of the two phases was required. Therefore, the phase separated entire flow field velocity measurement was performed using PIV-LIF. The velocity fields at three different sections, slug film, slug wake and slug nose, in a unit slug was measured and analyzed. It was found that the velocity of the gas phase in the film region was significantly higher than the liquid phase. As the bubble front penetrated into the liquid slugy body, it accelerated the liquid body and the velocity exchange was observed between the two phases. The vorticity and the interface shear stresses were measured and, as expected, were balanced at the interface between the two phases. In the film region, as the gas phase moved faster than the liquid, the slip velocity was high as was the vorticity while the interface shear stress remained low. In the wake section of the slug, the slip velocity decreased and the interface shear increased resulting in the increase of vorticity. The Proper Orthogonal Decomposition technique was applied to study turbulence and to visualize the complex structures embedded in the flow. The energy spectra for both phases were compared. The turbulent energy was mostly contained in the first three modes of the gas and liquid phase but the energy dissipated more rapidly in the liquid phase than the gas phase in a film region. This PIV-LIF technique, combined with POD is a powerful tool for studying two-phase (liquid-gas) flows and for studying the phase interaction and forces acting on the phases interface.

## Acknowledgement

This research has been supported by Yayasan Universiti Teknologi PETRONAS (YUTP).

## References

Published in Journal of Visualization
DOI 10.1007/s12650-015-0302-1
The final publication is available at link.springer.com

Adrian RJ, Westerweel J (2011) Particle Image Velocimetry. Cambridge.
Cai JY, Wang HW, Hong T, Jepson WP (1999) Slug frequency and length inclined large diameter multiphase pipeline, In: Proceedings of 4th International Symposium, Multiphase Flow and Heat Transfer, Xi'an China, 22-24 August, pp 195-202.
Carneiro JNE, Fonseca R Jr, Ortega AJ, Chucuya RC, Nieckele AO, Azevedo LFA (2011) Statistical Characterization of two-phase slug flow in a horizontal pipe. J. Braz. Soc. Mech. Sci. & Eng. 33: 251-258.
Czapp M, Muller C, Fernandez PA, Sattelmayer T (2012) High-Speed Stereo and 2D PIV Measurements of Two-phase Slug Flow in a Horizontal Pipe. In: 16th Int Symp on Applications of Laser Techniques to Fluid Mechanics Lisbon, Portugal, 09-12 July.
Fujiwara A, Danmoto Y, Hishida K, Maeda M (2004) Bubble deformation and flow structure measured by double shadow images and PIV/LIF. Exp Fluids 36:157-165.
Goharzadeh A, Rodgers P (2009) Experimental characterization of slug flow velocity distribution in two phase pipe flow. In: Proceedings of the ASME 2009 International Mechanical Engineering Congress & Exposition, IMECE2009, Florida, USA.
Jirka GH, Herlina H, Niepelt A (2010) Gas transfer at the air-water interface: experiments with different turbulence forcing mechanisms. Exp Fluids 49:319-327.
Kitagawa A, Hishida K, Kodama Y (2005) Flow structure of micro bubble-laden turbulent channel flow measured by PIV combined with the shadow image technique. Exp Fluids 38:466-475.
Lindken R, Merzkirch W (2002) A novel PIV technique for measurements in multiphase flows and its application to two-phase bubbly flows. Exp Fluids 33: 814-825.
Munir S, Heikal MR, Aziz ARA, Muthuvalu MS, Siddiqui MI (2014) Dynamical analysis of turbulent liquid phase in two-phase pipe flow. J. Science Asia, In Press.
Munir S, Heikal MR, Siddiqui MI, Aziz ARA, Muthuvalu MS (2014) Structure analysis of turbulent liquid phases by POD and LES techniques. In: 3rd International Conference on Fundamental and Applied Science 2014, AIP Conf. Proc. 1621, 116-122, DOI: http://dx.doi.org/10.1063/1.4898455
Milenković RŹ, Yadigaroglu G, Sigg B (2009) Study of interactions between liquid vortices and bubbles by simultaneous particle image velocimetry and laser-induced fluorescence tracking. Optics & Laser Technology 42:156-171.
Sirovich L (1987) Turbulence and the dynamic of coherent structures part 1-3. Q App Math 45: 561-590.
Siddiqui MI, Heikal MR, Munir S, Dass SC, Aziz ARA (2014) Influence of a gas bubble on the dynamical parameters of the slug flow using particle image velocimetry. In: 3rd International Conference on Fundamental and Applied Science 2014, AIP Conf. Proc. 1621, 691-698 (2014), DOI: http://dx.doi.org/10.1063/1.4898543
Sathe MJ, Thaker IH, Strand TE, Joshi JB (2009) Advanced PIV/LIF and shadowgraphy system to visualize flow structure in two-phase bubbly flows. Chem Eng Sci 65:2431-2442.
Yang B, Wang Y, Liu J (2011) PIV measurements of two phase velocity fields in Aeolian sediment transport using fluorescent tracer particles. Measurement 44:708-716.

Published in Journal of Visualization
DOI 10.1007/s12650-015-0302-1
The final publication is available at link.springer.com